Inviscid Two-Dimensional Fluid Dynamics Experiments with Magnetized Electron Columns

Joel Fajans and Daniel Durkin

Physics Dept, U.C. Berkeley, Berkeley CA 94720-7300, USA

1 Introduction

Inviscid two-dimensional (2D) fluid phenomena like hurricanes, jet streams, Jupiter's Red Spot, and protoplanetary disks are quite common in Nature. Unfortunately, 2D fluid phenomena are difficult to study in the laboratory because the finite size of laboratory apparati commonly introduces unwanted viscous and friction effects. Magnetized electron columns, however, behave like two-dimensional fluids and are not subject to viscous effects [1]. The columns behave like fluids because the equations which govern their behavior, the Drift-Poisson Equations, are identical to the 2D inviscid Euler equations which govern 2D fluids. More precisely, the columns follow $\boldsymbol{E} \times \boldsymbol{B}$ dynamics, i.e their velocity $\boldsymbol{v}$ is

$$\boldsymbol{v} = \boldsymbol{E} \times \boldsymbol{B}/B^2, \tag{1}$$

where $\boldsymbol{E}$ is the self-consistent electric field from the columns and any external potentials, and $\boldsymbol{B}$ is a strong external magnetic field. (The columns are trapped in a Malmberg-Penning trap; see Fig. 1.) The electric field can be derived from a potential, namely $\boldsymbol{E} = -\nabla\phi$. The vorticity is defined just as it would be for a fluid: $\Omega = \nabla \times \boldsymbol{v}$. Expressing the velocity in terms of the potential and using Poisson's equation yields

$$\Omega = \frac{e}{\epsilon_0 B} n, \tag{2}$$

where n is the electron density; thus vorticity is proportional to density. By creating electron columns with the appropriate density, we can model 2D fluid flows. To aid in the creation of arbitrary initial conditions, we have developed a photocathode source [2] that allows us to create any desired initial condition simply by projecting an appropriate light image onto the photocathode.

2 Decay of Turbulence

Magnetized plasma columns can be used to study the decay of 2D turbulence. For example, Fig. 2 shows the decay of a complicated initial vorticity distribution to a simple final state. The relaxation involves subprocesses like advection, instabilities, filamentation, merger, vortex in vortex interactions, and sometimes cooling into vortex crystals. Examples of each of these process will be given in this paper and more information can be found in the cited literature.

D. Reguera, L.L. Bonilla, and J.M. Rubí (Eds.): LNP 567, pp. 319–327, 2001.

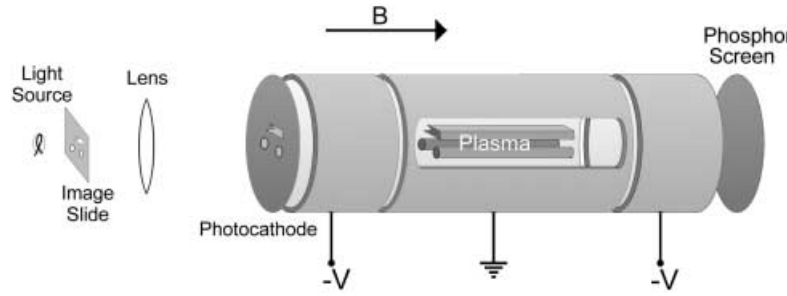

Fig. 1. Malmberg-Penning trap geometry. Negatively biasing the end cylinders provides axial confinement, and the axial magnetic field provides radial confinement. The electron columns (plasma) are emitted from the photocathode on the left, and loaded into the trap by temporarily grounding the left cylinder. The columns are diagnosed by grounding the right cylinder, thereby allowing the columns to stream out onto the phosphor screen. The images thus created are detected by a CCD camera. Movies of the evolution of the columns are obtained by successively regenerating the initial configuration and grounding the right cylinder at successively later times. Details of the trap operation can be found in Refs. [2,3].

2.1 Advection

Two vortices will interact with each other due to their mutual electric fields/stream functions. If the two vortices have the same sign, as in Fig. 3, the $\boldsymbol{E}$ fields from the two vortices will be radial but point in opposite directions. The resulting $\boldsymbol{E} \times \boldsymbol{B}$ velocities will be perpendicular to the $\boldsymbol{E}$ fields and point oppositely. As the vortices move, the $\boldsymbol{E}$ field directions will adjust; the end result is that the vortices will orbit around each other in a circle. If the two vortices have the opposite sign, the $\boldsymbol{E}$ fields will point in the same direction, and the vortices will drift together in the direction perpendicular to the line separating the vortices. For example, a vortex near a wall will move under the influence of its oppositely-signed image vortex; since the line connecting the original vortex and its image is radially directed, the drift direction will be azimuthal. Thus the vortex and its image will drift azimuthally, revolving around the trap wall [4]. Obviously electrons all have the same sign, so one might think that, aside from image vortices, magnetized electron columns would all have the same sign of vorticity, and it would be impossible to generate opposite sign vortices – anti-vortices. However, superimposing a uniform background density on a vorticity distribution is equivalent to transforming to a rotating frame, and such a transformation does not change the dynamics. In this rotating frame, the holes, i.e. the regions where the density is below the density of the uniform background, act exactly like anti-vortices. This point is illustrated in Fig. 4 which shows two holes revolving around each other until they merge. (Merger is discussed in Sec. 2.3.)

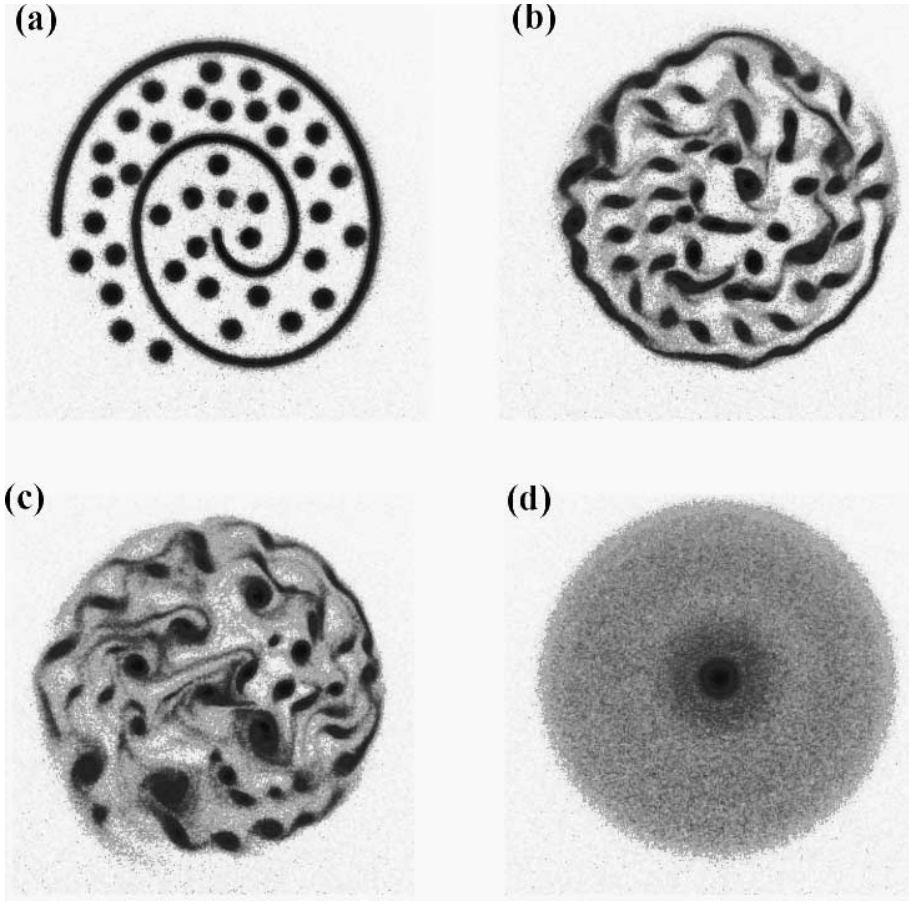

Fig. 2. An initially complicated state (a), evolving through successively simpler states (b-c) to a final relaxed state (d).

2.2 Filamentation

Several processes will induce filamentation. For example, a sufficiently elliptical vortex will spawn filaments from its tips (Fig. 5) [5]. More importantly, a strong vortex can rip apart a weak vortex (Fig. 6) [6]. Filamentation is important because it introduces fine scale structure that coarse graining, or the small, but unavoidable viscosity in the system will eventually smooth out. Typically this creates a tenuous background density/vorticity.

2.3 Merger

When two vortices of the same sign are sufficiently close to each other, they will merge into one larger vortex and several filaments. (See Fig. 4.) For identical

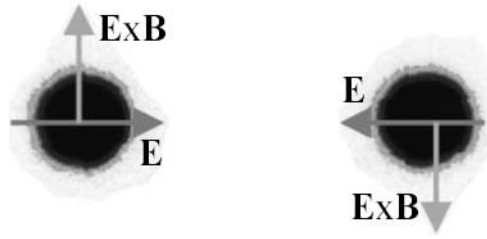

Fig. 3. Two vortices of the same sign. The left electric field arrow is the field from the right vortex, and vice versa. As the two electric fields are equal and opposite, the $\boldsymbol{E} \times \boldsymbol{B}$ velocities point azimuthally, and the two vortices orbit each other.

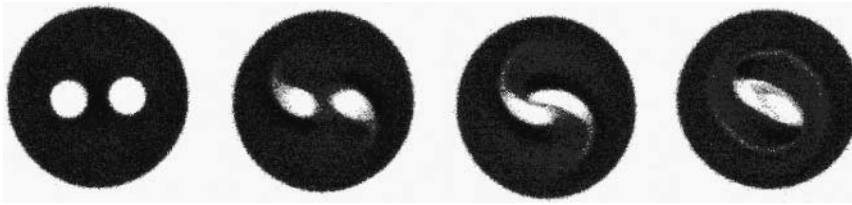

Fig. 4. The merger of two holes/anti-vortices.

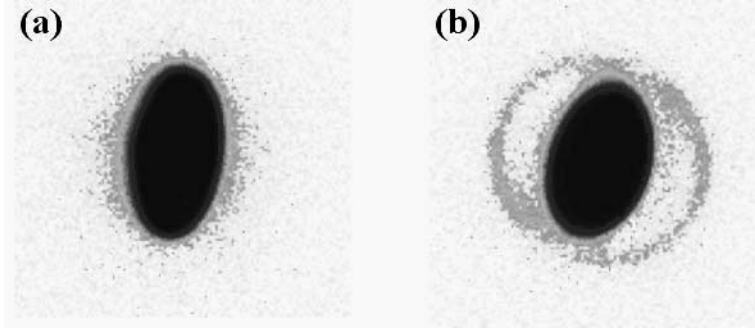

Fig. 5. An ellipse will spawn spiral filaments from its tips.

vortices, the precise merger criterion is that the centers of the two vortices must not be separated by more than 3.4 times the radius of the vortices. This process is very important to the decay of turbulence as it is the major mechanism by which discrete vortices aggregate. Merger was studied in detail by Fine, et. al [7].

2.4 Kelvin-Helmholtz Instabilities

A hollow ring of density/vorticity will be unstable to the Kelvin-Helmholtz instability (Fig. 7) [1]. The Kelvin-Helmholtz instability is due to shear in the

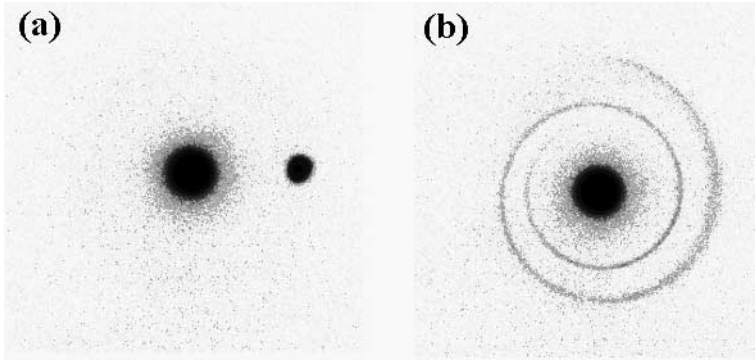

Fig. 6. A strong vortex will tear a weak vortex apart.

velocity; the inner edge of the ring moves slower than the outer edge. The number of lobes that the ring breaks up into is inversely proportional to the width of the ring [8,9]. More generally, any vorticity filament will be subject to this instability if the filament has sufficient shear.

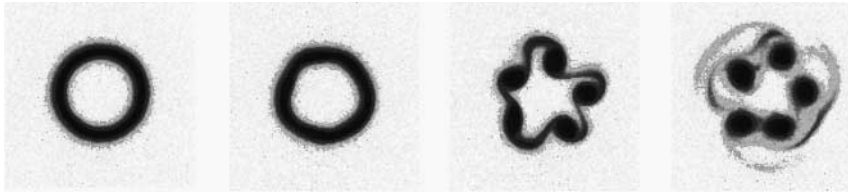

Fig. 7. The breakup of a hollow ring of vorticity/density due to the Kelvin-Helmholtz instability.

2.5 Vortex in Vortex Interactions

When a intense, point-like vortex is placed inside an diffuse, extended vortex, the point-like vortex will often induce a wave on the diffuse vortice's surface (Fig 8). The will grow nonlinearly and eventually break, entraining an anti-vortex. Depending on the parameters, the point vortex may be able to drag the anti-vortex into the extended vortice's interior. This interaction was only discovered very recently, and experimental measurements [10] are in good agreement with theoretical expectations [11]. The interaction's importance stems from the turbulence that it can engender in the initially relaxed extended vortex.

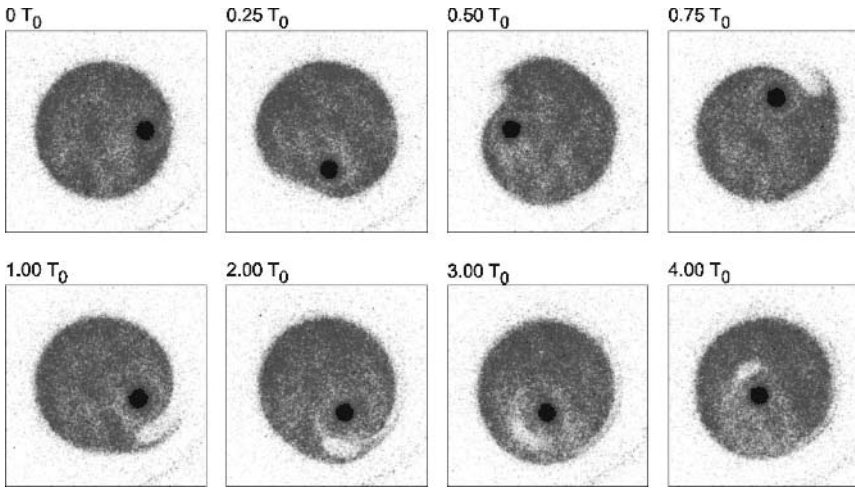

Fig. 8. Vortex in vortex interaction. The time T_0 is the time for the extended vortex to rotate once. The surface wave breaks at approximately $0.5T_0$, entrains an anti-vortex by $2T_0$, and the point vortex pulls the anti-vortex into the extended vortex interior by $3T_0$

2.6 Vortex Cooling and Crystallization

Interactions between initially randomly arranged vortices and an extended, diffuse background vortex will sometimes lead to the vortices cooling into a crystal [12,13,14,15]. A typical sequence is illustrated in Fig. 9, and a complex crystal is shown in Fig. 10 [16]. Figure 11 shows the measured "jitter" as a function of

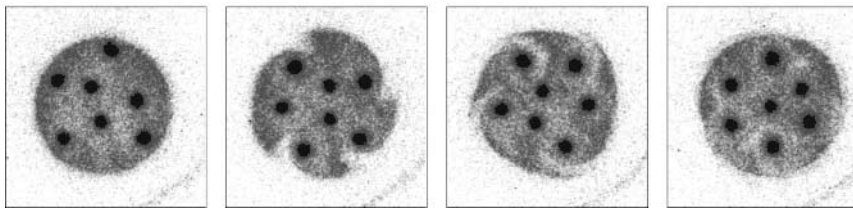

Fig. 9. An initially random configuration of seven vortices in a background cooling into a crystal.

time for a configuration of four randomly placed vortices in a background. The cooling results from the stirring of the background by the vortices. This maximizes the entropy of the background [19], producing a final state that favors crystallization. Computer simulations indicate that the cooling rate depends on the background density, with the fastest rates occuring for densities which are neither too high or too low [15]. However, typical computer simulations take

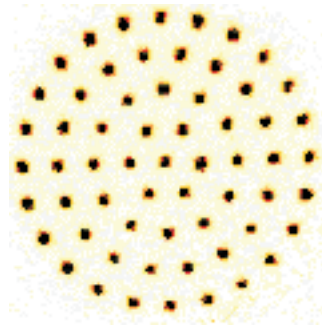

Fig. 10. A crystal with 61 vortices. This triangular lattice crystal is the fourth in a series of "magic" numbers, the first crystals having 7, 19 and 37 vortices. In this case, the crystal was created directly by the photocathode rather than by cooling from an initially random state. Vortex crystals have a long history; Lord Kelvin and J.J Thomson postulated that molecules might be stable configurations of vortices [17,18].

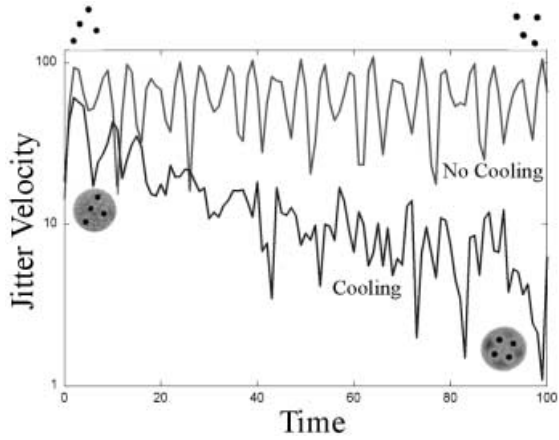

Fig. 11. Time vs. "Jitter Velocity" for two configuration: one with no background which does not cool, and one that is identical except for the addition of a background, which does cool. The Jitter Velocity is the velocity by which a configuration deviates from a uniform rotation.

many days, and only a limited number of initial conditions were explored. Our experimental measurements show that the cooling rate is at least as dependant on the closeness of the vortices to the background edge as it is on the background density.

2.7 Vortex Cooling and Unstable Equilibria

Sometimes the cooling process will take the system near an unstable equilibria; i.e. a crystal configuration that is unstable (Fig. 12). These unstable equilibria

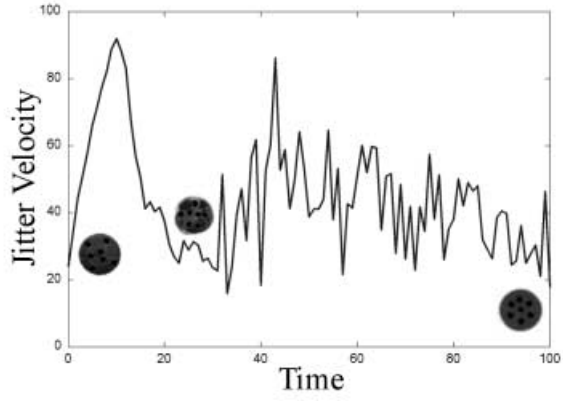

Fig. 12. Time vs. Jitter Velocity for the sequence of Fig. 9. Note how the system temporarily settles into what turns out to be an unstable equilibrium near a time of 25. The unstable equilibrium configuration is illustrated by the middle small inset figure; the final stable configuration is illustrated by the inset figure on the right.

were recently predicted by Aref and Vainchtein [20] who correctly assert that the system will stagnate in the vicinity of an unstable equilibrium.

3 Conclusions

Magnetized plasma columns are a powerful tool to study 2D fluid dynamics. In conjunction with analytic work and computer simulations, magnetized electron columns can be used to study many theoretical issues as well as problems in Nature. Our recently developed photocathode source, which allows us to create arbitrary initial conditions, greatly extends the range of experiments that can be undertaken.

Acknowledgments

Many people contributed to this work at Berkeley, including E.Yu. Backhaus, R. Chu, E. Gilson, J. Notte, A.J. Peurrung, J. Siegel, J.S. Wurtele, and L. Zimmerman. Experimentalists cited at other institutions include C.F. Driscoll and K. Fine at UCSD, and D.L. Eggleston at Occidental. This work was supported by the Office of Navel Research.

References

1. R. H. Levy, Phys. Fluids **8**, 1288 (1965).
2. D. Durkin and J. Fajans, Rev. Sci. Instrum. **70**, 4539 (1999).

3. J. H. Malmberg, C. F. Driscoll, B. Beck, D. L. Eggleston, J. Fajans, K. Fine, X. P. Huang, and A. W. Hyatt, in *Nonneutral Plasma Physics*, edited by C. Roberson and C. Driscoll (American Institute of Physics, New York, 1988), Vol. AIP 175, p. 28.
4. W. D. White, J. H. Malmberg, and C. F. Driscoll, Phys. Rev. Lett. **49**, 1822 (1982).
5. M. V. Melander, N. J. Zabusky, and J. C. McWilliams, J. Fluid Mech. **195**, 303 (1988).
6. D. L. Eggleston, Phys. Plasmas **1**, 3850 (1995).
7. K. S. Fine, C. F. Driscoll, J. H. Malmberg, and T. B. Mitchell, Phys. Rev. Lett. **67**, 588 (1991).
8. A. J. Peurrung and J. Fajans, Phys. Fluids A **5**, 493 (1993).
9. A. J. Peurrung, J. Notte, and J. Fajans, J. Fluid Mech. **252**, 713 (1993).
10. D. Durkin and J. Fajans, submitted to Phys. Rev. Lett.
11. D.Z. Jin and D.H.E. Dubin, submitted to Phys. Plasmas.
12. T. Havelock, Philos. Mag. **11**, 617 (1931).
13. L. Campbell and R. Ziff, A Catalog of Two-Dimensional Vortex Patterns, Los Alamos Scientific Laboratory Report No. LA-7384-MS, 1978.
14. K. Fine, A. Cass, W. Flynn, and C. Driscoll, Phys. Rev. Lett. **75**, 3277 (1995).
15. D. A. Schecter, D. H. E. Dubin, K. S. Fine, and C. F. Driscoll, Phys. Fluids **11**, 905 (1999).
16. D. Durkin and J. Fajans, Phys. Fluids **12**, 298 (2000).
17. W. T. Kelvin, *Mathematical and Physical Papers, iv.* (Cambridge University Press, Cambridge, 1878), p. 135.
18. J. Thomson, *Treatise on Vortex Rings* (Macmillan, London, 1883), p. 94.
19. D. Z. Jin and D. H. E. Dubin, Phys. Rev. Lett. **80**, 4434 (1998).
20. H. Aref and D. Vainchtein, Nature **392**, 769 (1998).